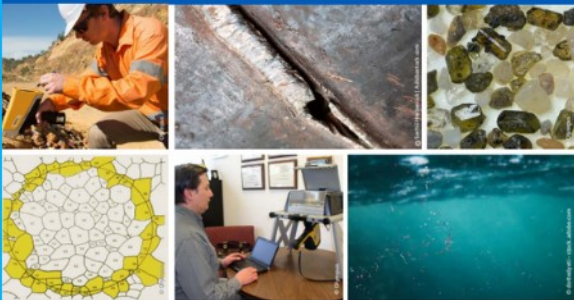




2nd Advanced Optical Metrology Compendium

Advanced Optical Metrology

Geoscience | Corrosion | Particles | Additive Manufacturing: Metallurgy, Cut Analysis & Porosity



EVIDENT
OLYMPUS

WILEY

The latest eBook from **Advanced Optical Metrology**.
Download for free.

This compendium includes a collection of optical metrology papers, a repository of teaching materials, and instructions on how to publish scientific achievements.

With the aim of improving communication between fundamental research and industrial applications in the field of optical metrology we have collected and organized existing information and made it more accessible and useful for researchers and practitioners.

EVIDENT
OLYMPUS

WILEY

Fluorobenzene and Water-Promoted Rapid Growth of Vertical Graphene Arrays by Electric-Field-Assisted PECVD

Chao Shen, Shichen Xu, Zhuo Chen, Nannan Ji, Jinhui Yang,* and Jin Zhang*

Vertical graphene (VG) arrays show exposed sharp edges, ultra-low electrical resistance, large surface-to-volume ratio, and low light reflectivity, thus having great potential in emerging applications, including field emission, sensing, energy storage devices, and stray light shields. Although plasma enhanced chemical vapor deposition (PECVD) is regarded as an effective approach for the synthesis of VG, it is still challenging to increase the growth rate and height of VG arrays simultaneously. Herein, a fluorobenzene and water-assisted method to rapidly grow VG arrays in an electric field-assisted PECVD system is developed. Fluorobenzene-based carbon sources are used to produce highly electronegative fluorine radicals to accelerate the decomposition of methanol and promote the growth of VG. Water is applied to produce hydroxyl radicals in order to etch amorphous carbon and accelerate the VG growth. The fastest growth rate can be up to $15.9 \mu\text{m h}^{-1}$. Finally, VG arrays with a height of $144 \mu\text{m}$ are successfully synthesized at an average rate of $14.4 \mu\text{m h}^{-1}$. As a kind of super black material, these VG arrays exhibit an ultra-low reflectance of 0.25%, showing great prospect in stray light shielding.

VG can be easily obtained through top-down methods using graphene oxide (GO), the presence of impurities and oxygen-containing functional groups in GO can significantly cause phonon scattering and electronic structure changing, thus significantly affecting the thermal and electrical properties and especially causing serious impact on their related applications. By contrast, bottom-up methods represented by plasma enhanced chemical vapor deposition (PECVD) can directly grow VG in one step, which enables to retain the intrinsic properties of graphene.^[6,13] Owing to these advantages, PECVD has been considered as a promising and controllable technique to fabricate VG.

As a significant method for producing carbon materials including diamonds, carbon nanotubes (CNTs),^[14,15] graphene,^[16] and especially VG, PECVD

system can be classified into many types according to the plasma sources, such as direct current (DC) sources,^[17] radio frequencies (RF) sources, microwave (MW) sources,^[18,19] and combinations of the aforementioned types. Due to high electron energy and density, low growth temperature, and simple growth equipment, RF-PECVD is regarded as an effective method to prepare VG. However, RF-PECVD still faces the difficulty in rapid and vertically oriented growth of VG. By introducing built-in electric field into RF-PECVD, our group has realized the controlled preparation of graphene sheets strictly perpendicular to the substrates.^[11] However, accelerating its growth rate is still a very difficult problem. Many catalysts and carbon sources were introduced into the RF-PECVD system to promote the growth of VG.^[6,11,20] Nonetheless, it still took hours to synthesize VG with a height of several microns, which restricts the widespread applications of VG. Therefore, rapid growth of ultrahigh VG with controllable orientation is of vital importance.

Herein, we developed a fluorobenzene and water-assisted method for the growth of VG arrays in electric field-assisted RF-PECVD system. Under the effect of highly electronegative fluorine radicals decomposed from fluorobenzene, the fastest growth rate of VG arrays in our system could be increased by three times from 3.6 to $11.2 \mu\text{m h}^{-1}$. Furthermore, the fastest growth rate of VG arrays can be further increased to $15.9 \mu\text{m h}^{-1}$ when an appropriate proportion of water was introduced into growth system to etch amorphous carbon. The height of the VG arrays can reach $144 \mu\text{m}$. Finally, as a super black material, the


1. Introduction

Different from horizontal graphene films, vertical graphene (VG) arrays possess a special structure, including non-stacking morphology, exposed sharp edges, low reflectance, and great mechanical stabilities.^[1] Due to these excellent properties, VG arrays have become the most promising material for application in super black materials,^[2,3] field emission devices,^[4,5] and supercapacitors.^[6] To fulfill the increasing demand for VG, various preparation methods have been successively developed, including top-down^[7,8] and bottom-up^[9–12] methods. Although

C. Shen, J. Yang
College of Chemistry and Chemical Engineering
Ningxia University
Yinchuan 750021, P. R. China
E-mail: yang_jh@nxu.edu.cn

C. Shen, S. Xu, Z. Chen, N. Ji, J. Zhang
Beijing Graphene Institute (BGI)
Beijing 100095, P. R. China

S. Xu, J. Zhang
College of Chemistry and Molecular Engineering
Peking University
Beijing 100871, P. R. China
E-mail: jinzhang@pku.edu.cn

 The ORCID identification number(s) for the author(s) of this article can be found under <https://doi.org/10.1002/sml.202207745>.

DOI: 10.1002/sml.202207745

as-grown VG arrays exhibited an ultralow reflectance of $<0.25\%$ in the visible light region, showing great potential in applications of stray light masks, energy collection, and bolometer.

2. Results and Discussion

Figure 1a schematically illustrates the process for preparing VG arrays by fluorobenzene and water-assisted PECVD system. The electric-field-assisted PECVD setup is shown in Figure S1, Supporting Information. Under the combined effect of high temperature, plasma bombardment, and fluorine radicals, methanol can be decomposed into various radicals. Meanwhile, water is introduced in the system to etch amorphous carbon. The structure of VG arrays is revealed by SEM (Figure 1b). The height of VG arrays grown in our PECVD system reaches $143.9\ \mu\text{m}$ with an average growth rate of $14.4\ \mu\text{m h}^{-1}$. The intensity ratio of D peak to G peak is 1.02 and intensity ratio of 2D peak to G peak is 0.60 in the Raman spectra (Figure 1c). Figure 1d exhibits the height of graphene grown by the conventional RF-PECVD and our method as a function of time, where the slope represents the average growth rate of VG. It can be found that most VG has a slow growth rate and limited height. Compared with VG arrays produced by conventional RF-PECVD method, VG arrays grown by fluorobenzene and water-assisted RF-PECVD have superior advantages in growth rate, height, and morphology (Figure S2 and Table S1, Supporting Information).

2.1. The Effect of Fluorobenzene

In the PECVD process, carbon sources are decomposed under the effect of plasma. Then radicals, which are pivotal factors to grow VG such as C_2 , CH, and H, are generated. Since halogen radical possesses a strong electronegativity, it can easily facilitate carbon sources dehydrogenation reaction.^[21,22] Herein, fluorobenzene is chosen to promote the decomposition of methanol. The effect of fluorobenzene is schematically illustrated in Figure 2a. The energy generated by the plasma is high enough to decompose the fluorobenzene into fluorine radicals effectively. The fluorine radicals can help carbon sources decompose into active radicals, and this is followed by the nucleation and growth of VG.^[21–23] Figure 2b,c show that after the introduction of fluorobenzene, the height of VG arrays is strongly increased. As shown in Figure 2d and Figure S3, Supporting Information, the growth rate of VG arrays gradually increases with the ratio of fluorobenzene to methanol increasing and reaches the fastest rate of $11.2\ \mu\text{m h}^{-1}$ when the optimum ratio is 1:5. With further increase of the ratio of fluorobenzene to methanol, the growth rate of VG arrays significantly slows down. This is because too much amorphous carbon generated by extra active carbon species will be absorbed on the open edge of VG, so that the growth of VG is inhibited.

In situ optical emission spectrum (OES) is used to reveal the growth mechanism of two different systems. Although C_2 , OH, CH, and H peaks can be found in both systems with and

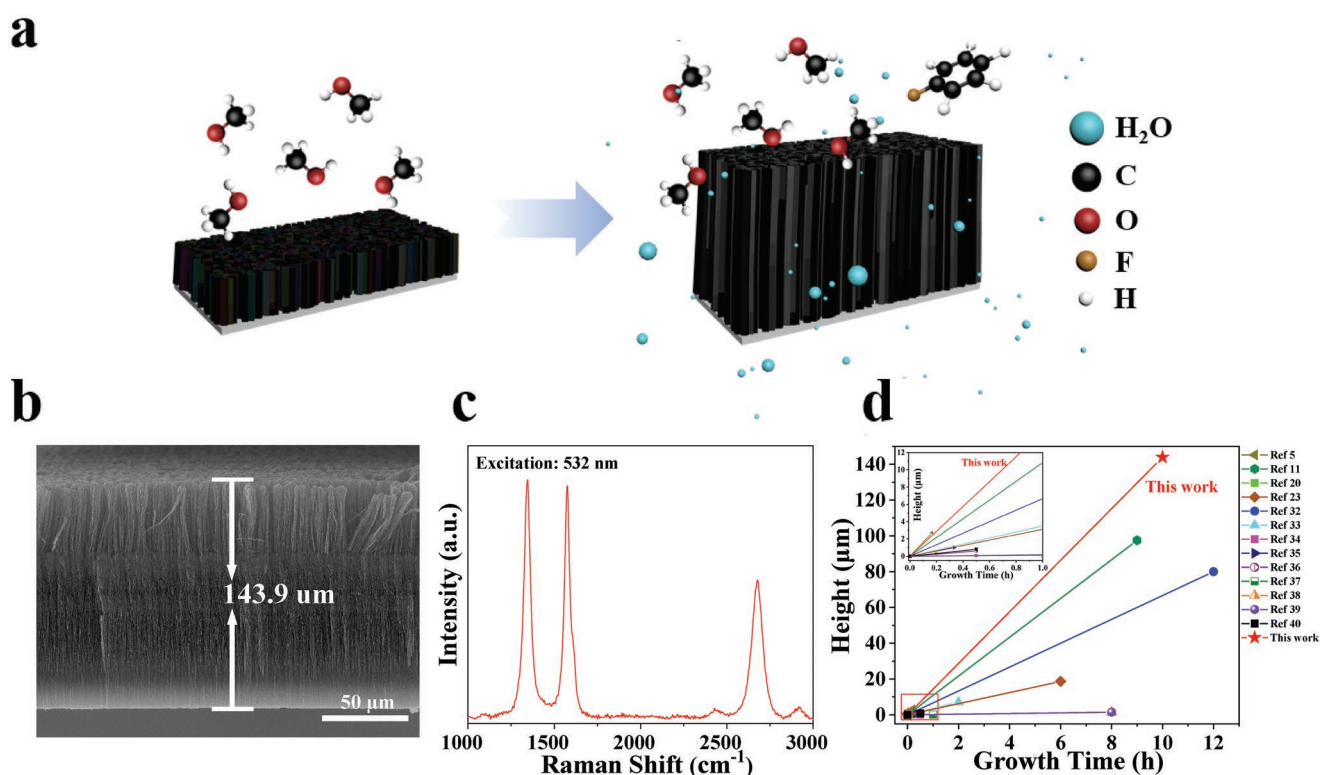


Figure 1. Fluorobenzene and water assisted synthesis process and growth results of VG. a) Schematic illustrating the growth procedure of VG arrays in fluorobenzene and water system. b) Cross-sectional SEM image of VG arrays after 10 h growth. c) Raman spectrum of VG arrays. d) Comparison of height, average growth rate, and morphology of VG between our work and previous works using traditional RF-PECVD methods. The slope represents the average growth rate.

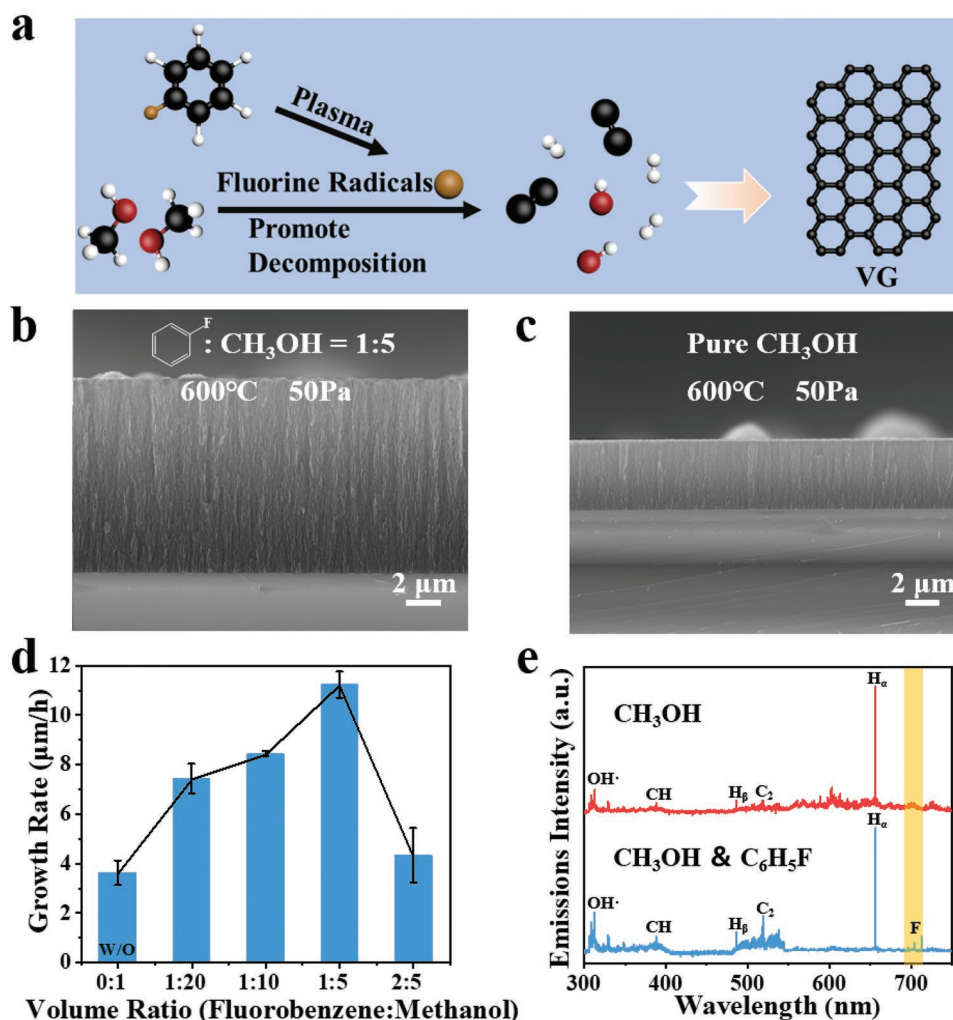


Figure 2. Rapid growth of VG arrays assisted by fluorobenzene. a) Schematic illustrating the growth procedure of VG arrays in fluorobenzene system. b) Sectional SEM images of VG arrays grown with fluorobenzene. c) Sectional SEM images of VG arrays grown without fluorobenzene. d) Volume ratio of fluorobenzene to methanol on VG arrays growth. e) In situ OES spectra of the reaction systems.

without fluorobenzene, the signal of fluorine at 696.6, 703.7, and 639.9 nm can only be detected in the fluorobenzene-based carbon sources system (Figure 2e).^[23–25] The ratios of OH peak to H_α peak (0.34) and C₂ peak to H_α peak (0.32) in fluorobenzene system are much higher than the ratios of OH peak to H_α peak (0.20) and C₂ peak to H_α peak (0.12) in non-fluorobenzene system, respectively. Usually, the more C₂ radicals, the faster the VG grows.^[26,27] In addition, the rapid growth of VG arrays was attributed to the present of fluorine element, which can directly react with methanol to promote the dehydrogenation reaction of carbon sources.

2.2. The Effect of Water

Hydroxyl radical is an excellent etching agent in the growth of various carbon materials.^[28–31] Normally, hydroxyl radical is produced from the alcohol-based carbon source by bombardment of plasma and pyrolysis of high temperature. However, hydroxyl radicals generated from methanol carbon source are

not enough to etch amorphous carbon in high carbon density in our fluorobenzene-based PECVD system. Therefore, water is chosen to produce more hydroxyl radicals. **Figure 3a** schematically illustrates the etching mechanism of water during VG growth. In the process of VG growth, some amorphous carbon can be absorbed on both the VG surface and open edge which could result in the decline of growth rate and defects of VG. Therefore, hydroxyl radicals generated by plasma and high temperature can help remove the amorphous carbon, thus remaining the growth activity of VG. Figure 3b and Figure S4, Supporting Information, show that the growth rate of VG arrays gradually increases and reaches a peak of 15.9 µm h⁻¹ with the increase of water. After that, the growth rate gradually decreases, which indicates too much water will inhibit the growth of VG arrays. As is shown in Figure 3c and Figure S5, Supporting Information, after introduction of water, all of the growth rate of VG arrays can be increased using carbon sources with different volume ratios of fluorobenzene to methanol. Moreover, the I_D/I_G of VG produced under high-concentration carbon source decreases gradually with the increase of the

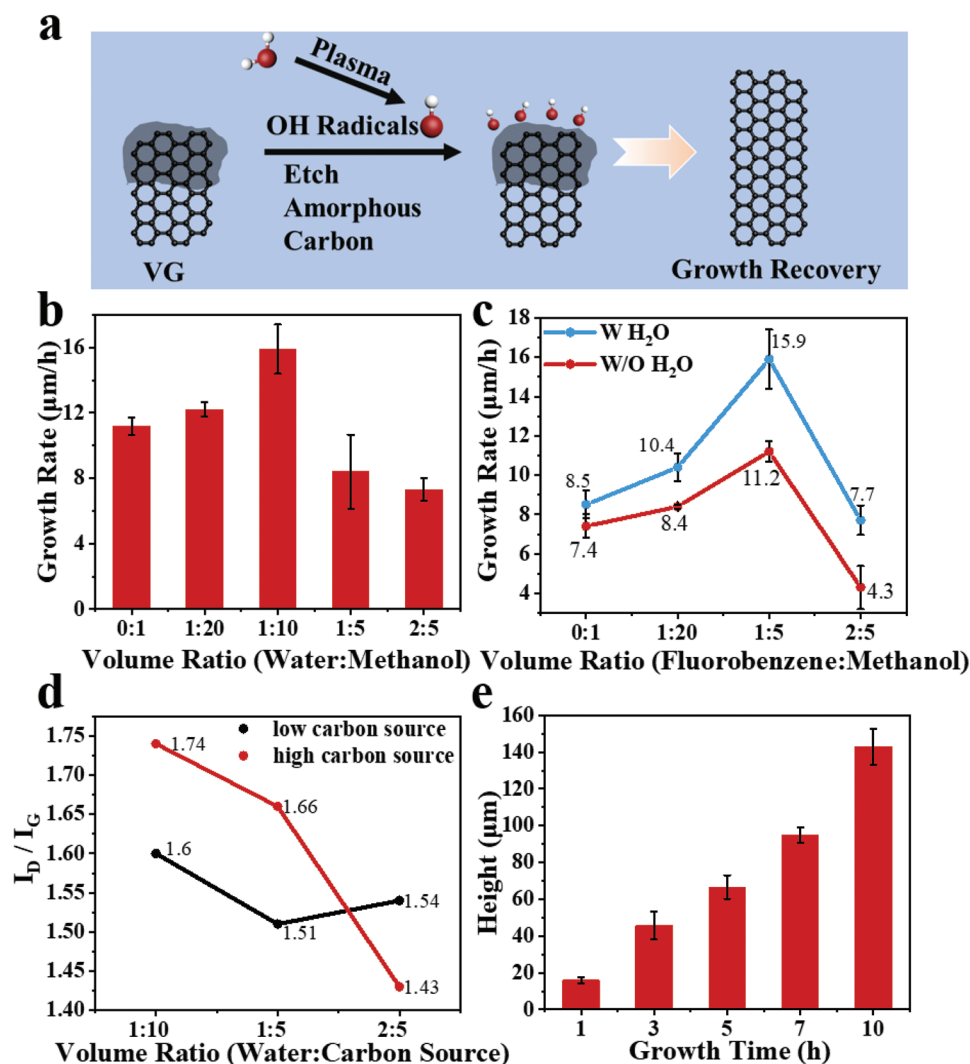


Figure 3. Rapid growth of VG arrays assisted by water. a) Schematic illustrating the growth procedure of VG arrays in water system. b) The relationship between the growth rate of the VG arrays and the volume ratio of water and methanol, under the ratio of 1:5 fluorobenzene to methanol. c) Line chart comparing the heights of VG arrays grown with and without water versus volume ratio of fluorobenzene to methanol. d) Line chart comparing the I_D/I_G of VG arrays grown with high carbon source and low carbon source versus volume ratio of water to methanol. e) Histogram comparing the heights of VG arrays grown with different time.

water ratio, indicating that the quality of VG becomes higher. However, when the low-concentration carbon source is applied, the I_D/I_G does not decrease significantly, but increases slightly (Figure 3d). In the low-concentration carbon source system, due to less amorphous carbon during VG growth, the hydroxyl radicals generated by a large amount of water will dilute the active carbon radicals, then inhibit the growth of VG and introduce some defects in VG sheets. Figure 3e and Figure S6, Supporting Information, show there is a linear relationship between the height of VG arrays and growth time, more importantly VG arrays at a height of 144 μm are prepared within 10 h.^[32–40] Figure S7, Supporting Information, shows that the sheet resistance of VG arrays gradually decreases and tends to be stable with the increase of growth time, and Figure S8, Supporting Information, reveals an obvious disparity of surface wettability between VG glass and bare glass. Further, the contact angle values show a gradual increase with the extension of

CVD growth time and reaching 149.2° for 60 min growth. Such a surface hydrophobicity of VG arrays is of great practical significance for self-cleaning applications. Furthermore, both SEM elemental analysis and XPS show that the VG is free of fluorine, which means that fluorine only plays an important role in gas reaction for rapid growth of VG arrays (Figure S9, Supporting Information).

2.3. Application of VG Arrays

Experiments have verified the universality of our method to grow VG arrays, and ultra-black VG arrays can be obtained on different substrates, including copper foil, iron foil, silicon wafer, and graphite paper (Figure 4a). As a matter of fact, the interaction between light and porous material can be divided into three categories according to the different feature sizes of

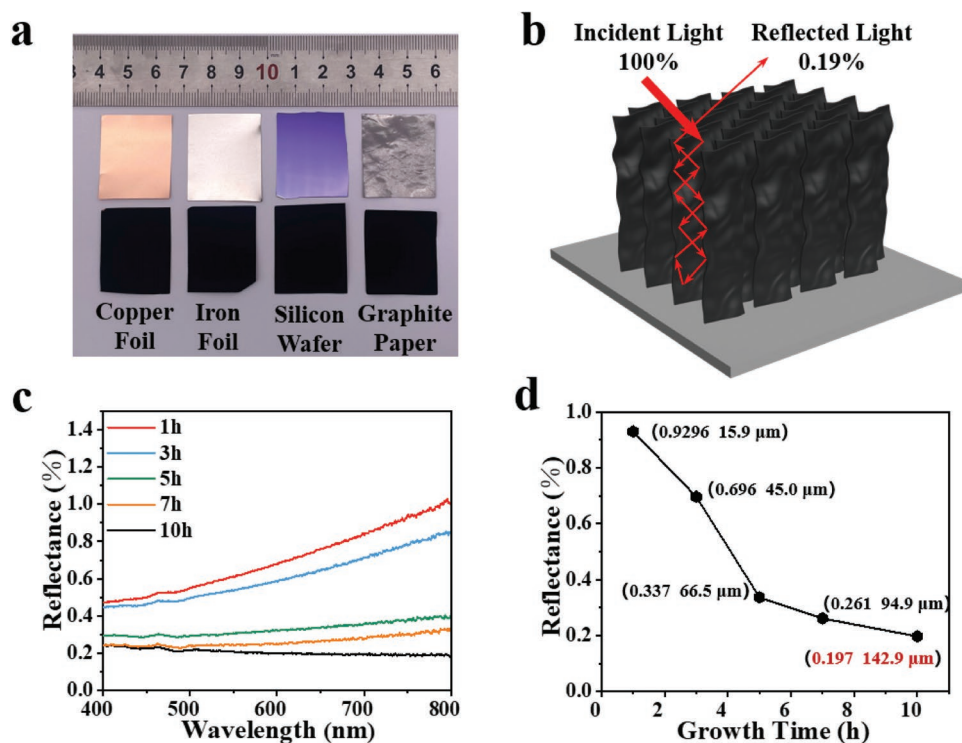


Figure 4. a) Photograph of VG arrays grown on various substrates. b) Schematic diagram showing the light reflectivity of VG arrays. c) Series of hemispherical reflectance spectra of VG arrays samples. d) The hemispherical reflectance of VG arrays grown for different times.

pores: pores with the dimensions much larger than the light wavelength, pores with dimensions in the same scale as the light wavelength, and pores with the dimensions much smaller than the light wavelength. Among them, reflectivity can be minimized when the gap between arrays has the same dimension as the light wavelength. At this point, the light can be trapped in the gap, resulting in multiple internal reflections, which are eventually fully absorbed.^[41,42] For our system, the pores between our graphene arrays are no more than 1 μm and even can be as small as 100 nm (Figure S10, Supporting Information), which are in the same scale of visible wavelengths (400–800 nm), therefore the reflectivity in the visible range can reach a very low level. As illustrated in Figure 4b, light on the VG arrays is trapped in the gap between VG sheets, and the light is completely absorbed by the VG array after multiple internal reflections ultimately making the reflectance of VG extremely low. Compared to VG arrays with a height of several micrometers, the incident light in VG arrays with a height of 100 μm will be reflected, refracted, and absorbed many times, resulting in a low reflectivity (Figure S11, Supporting Information). As shown in Figure 4c and Figure S12, Supporting Information, the hemispherical reflectance in the visible spectral and near IR regions are measured for the VG arrays samples with different growth time. There is a gradual decrease in reflectance when growth time is prolonged and it is remarkable that for VG arrays with 10 h growth the reflectance reaches up to 0.19% at a wavelength of 700 nm. Furthermore, Figure 4d shows the growth time-dependent hemispherical reflectance. With the increase of growth time, the reflectivity of VG arrays gradually decreases and tends to be stable. In addition, the difference in

reflectivity of VG on different substrates is very small (Figure S13, Supporting Information).

3. Conclusion

In this study, we developed a double-enhanced method for rapid growth of VG arrays. Using this method, the growth rate and height of VG arrays in the PECVD system were directly enhanced by introducing fluorobenzene and water. Among them, fluorobenzene promoted carbon source decomposing and water etched amorphous carbon, which both accelerated the growth of VG arrays. Finally, the fastest growth rate can be up to 15.9 $\mu\text{m h}^{-1}$. When the appropriate volume ratio of fluorobenzene and water were introduced into methanol carbon source, the height of VG arrays could reach 144 μm at an average growth rate of 14.4 $\mu\text{m h}^{-1}$. In addition, the total reflectance of VG arrays can reach up to 0.19% because most of the light was trapped in the deep gap of VG arrays, and VG arrays prepared by this catalyst-free method were expected to become an ideal super black material. Due to the catalyst-free growth conditions, low reflectivity, and fast growth rate, the resultant super black material shows a great potential to be applied onto stray light shields.

4. Experimental Section

Preparation of VG Arrays: A conventional inductively coupled PECVD with a built-in electric field was used to grow VG arrays. The frequency of radio frequencies sources were 13.56 MHz, and the electric field

was generated by two electrodes connected by a DC power source. In brief, different substrates were placed in the heating zone of the tube furnace after cleaning. The growth temperature and the voltage were set at 600 °C and 100 V, respectively. Methanol, fluorobenzene, and water were then fed into the PECVD system with an RF power of 250 W. In our system, the rotor flowmeter can strictly control the flow of carbon source and fluorobenzene/water to a certain extent. The pressure of the system is 50 Pa. After introducing an in-built electric field, VG can start growing.

Characterization: The morphology and detailed structure of VG arrays were investigated by SEM (FEI Quattro S, acceleration voltage 5–10 kV), Raman spectroscopy (Horiba, LabRAM HR 800, 532 nm laser wavelength), XPS (Kratos Analytical Axis-Ultra spectrometer with Al K α X-ray source). Under normal incident light, the optical reflectivity was measured with a UV–vis–NIR spectrometer (Lambda 950, USA).

Supporting Information

Supporting Information is available from the Wiley Online Library or from the author.

Acknowledgements

C.S. and S.X. contributed equally to this work. This work was partially supported by the Ministry of Science and Technology of China (2016YFA0200100 and 2018YFA0703502), the National Natural Science Foundation of China (Grant Nos. T2188101, 52021006, 51720105003, 21790052, and 21974004), the Strategic Priority Research Program of CAS (XDB36030100), and the Beijing National Laboratory for Molecular Sciences (BNLMS-CXTD-202001).

Conflict of Interest

The authors declare no conflict of interest.

Data Availability Statement

The data that support the findings of this study are available from the corresponding author upon reasonable request.

Keywords

fluorobenzene assisted rapid growth, super black materials, vertical graphene arrays, water assisted rapid growth

Received: December 11, 2022

Published online:

- [1] Z. Bo, S. Mao, Z. J. Han, K. F. Cen, J. H. Chen, K. Ostrikov, *Chem. Soc. Rev.* **2015**, *44*, 2108.
- [2] K. Davami, J. Cortes, N. Hong, I. Bargatin, *Mater. Res. Bull.* **2016**, *74*, 226.
- [3] S. Evlashin, S. Svyakhovskiy, N. Suetin, A. Pilevsky, T. Murzina, N. Novikova, A. Stepanov, A. Egorov, A. Rakhimov, *Carbon* **2014**, *70*, 111.
- [4] Y. Zhang, J. Du, S. Tang, P. Liu, S. Deng, J. Chen, N. Xu, *Nanotechnology* **2012**, *23*, 015202.

- [5] M. Y. Zhu, R. A. Outlaw, M. Bagge-Hansen, H. J. Chen, D. M. Manos, *Carbon* **2011**, *49*, 2526.
- [6] S. Xu, M. Wu, J. Zhang, *Chem. - Eur. J.* **2022**, *28*, 202200237.
- [7] F. An, X. F. Li, P. Min, P. F. Liu, Z. G. Jiang, Z. Z. Yu, *ACS Appl. Mater. Interfaces* **2018**, *10*, 17383.
- [8] W. Dai, T. F. Ma, Q. W. Yan, J. Y. Gao, X. Tan, L. Lv, H. Hou, Q. P. Wei, J. H. Yu, J. B. Wu, Y. G. Yao, S. Y. Du, R. Sun, N. Jiang, Y. Wang, J. Kong, C. P. Wong, S. Maruyama, C. T. Lin, *ACS Nano* **2019**, *13*, 11561.
- [9] X. H. Xia, S. J. Deng, D. Xie, Y. D. Wang, S. S. Feng, J. B. Wu, J. P. Tu, *J. Mater. Chem.* **2018**, *6*, 15546.
- [10] D. Xie, X. H. Xia, Y. Zhong, Y. D. Wang, D. H. Wang, X. L. Wang, J. P. Tu, *Adv. Energy Mater.* **2021**, *11*, 1601804.
- [11] S. C. Xu, S. Wang, Z. Chen, Y. Sun, Z. Gao, H. Zhang, J. Zhang, *Adv. Funct. Mater.* **2020**, *30*, 2003302.
- [12] S. C. Xu, Y. Y. Wen, Z. Chen, N. N. Ji, Z. G. Zou, M. M. Wu, L. T. Qu, J. Zhang, *Angew. Chem., Int. Ed.* **2021**, *60*, 24505.
- [13] K. Wang, S. Cheng, Q. Hu, F. Yu, Y. Cheng, K. Huang, H. Yuan, J. Jiang, W. Li, J. Li, S. Xu, J. Yin, Y. Qi, Z. Liu, *Nano Res.* **2021**, *15*, 9727.
- [14] Z. F. Ren, Z. P. Huang, J. W. Xu, J. H. Wang, P. Bush, M. P. Siegal, P. N. Provencio, *Science* **1998**, *282*, 1105.
- [15] P. He, Z. Ding, X. Zhao, J. Liu, Q. Huang, J. Peng, L. Z. Fan, *Carbon* **2019**, *155*, 453.
- [16] Y. Qi, B. Deng, X. Guo, S. Chen, J. Gao, T. Li, Z. Dou, H. Ci, J. Sun, Z. Chen, R. Wang, L. Cui, X. Chen, K. Chen, H. Wang, S. Wang, P. Gao, M. H. Rummeli, H. Peng, Y. Zhang, Z. Liu, *Adv. Mater.* **2018**, *30*, 201704839.
- [17] H. N. Ci, H. Y. Ren, Y. Qi, X. D. Chen, Z. L. Chen, J. C. Zhang, Y. F. Zhang, Z. F. Liu, *Nano Res.* **2018**, *11*, 3106.
- [18] N. G. Shang, P. Papakonstantinou, M. McMullan, M. Chu, A. Stamboulis, A. Potenza, S. S. Dhesi, H. Marchetto, *Adv. Funct. Mater.* **2008**, *18*, 3506.
- [19] Q. Yan, F. E. Alam, J. Gao, W. Dai, X. Tan, L. Lv, J. Wang, H. Zhang, D. Chen, K. Nishimura, L. Wang, J. Yu, J. Lu, R. Sun, R. Xiang, S. Maruyama, H. Zhang, S. Wu, N. Jiang, C. T. Lin, *Adv. Funct. Mater.* **2021**, *31*, 2104062.
- [20] Y. Ma, H. Jang, S. J. Kim, C. Pang, H. Chae, *Nanoscale Res. Lett.* **2015**, *10*, 308.
- [21] Y. Xie, T. Cheng, C. Liu, K. Chen, Y. Cheng, Z. Chen, L. Qiu, G. Cui, Y. Yu, L. Cui, M. Zhang, J. Zhang, F. Ding, K. Liu, Z. Liu, *ACS Nano* **2019**, *13*, 10272.
- [22] C. Liu, X. Z. Xu, L. Qiu, M. H. Wu, R. X. Qiao, L. Wang, J. H. Wang, J. J. Niu, J. Liang, X. Zhou, Z. H. Zhang, M. Peng, P. Gao, W. L. Wang, X. D. Bai, D. Ma, Y. Jiang, X. S. Wu, D. P. Yu, E. G. Wang, J. Xiong, F. Ding, K. H. Liu, *Nat. Chem.* **2019**, *11*, 730.
- [23] S. Kondo, M. Hori, K. Yamakawa, S. Den, H. Kano, M. Hiramatsu, *J. Vac. Sci. Technol., B: Microelectron. Nanometer Struct.–Process., Meas., Phenom.* **2008**, *26*, 1294.
- [24] G. Hancock, J. P. Sucksmith, *J. Vac. Sci. Technol., A* **2002**, *20*, 270.
- [25] M. F. Cuddy, E. R. Fisher, *J. Appl. Phys.* **2010**, *108*, 033303.
- [26] Z. Y. Qiu, P. Li, Z. Y. Li, J. L. Yang, *Acc. Chem. Res.* **2018**, *51*, 728.
- [27] Y. Sun, L. Yang, K. Xia, H. Liu, D. Han, Y. Zhang, J. Zhang, *Adv. Mater.* **2018**, *30*, 1803189.
- [28] L. Ding, A. Tselev, J. Y. Wang, D. N. Yuan, H. B. Chu, T. P. McNicholas, Y. Li, J. Liu, *Nano Lett.* **2009**, *9*, 800.
- [29] Y. Wang, Y. Q. Liu, X. L. Li, L. C. Cao, D. C. Wei, H. L. Zhang, D. C. Shi, G. Yu, H. Kajiura, Y. M. Li, *Small* **2007**, *3*, 1486.
- [30] H. P. Wang, X. D. Xue, Q. Q. Jiang, Y. L. Wang, D. C. Geng, L. Cai, L. P. Wang, Z. P. Xu, G. Yu, *J. Am. Chem. Soc.* **2019**, *141*, 11004.
- [31] S. J. Wei, L. P. Ma, M. L. Chen, Z. B. Liu, W. Ma, D. M. Sun, H. M. Cheng, W. C. Ren, *Carbon* **2019**, *148*, 241.
- [32] J. Han, Y. Ma, M. Wang, L. Li, Z. Tong, L. Xiao, S. Jia, X. Chen, *ACS Appl. Mater. Interfaces* **2021**, *13*, 12400.

- [33] Y. Ma, W. Jiang, J. Han, Z. Tong, M. Wang, J. Suhr, X. Chen, L. Xiao, S. Jia, H. Chae, *ACS Appl. Mater. Interfaces* **2019**, *11*, 10237.
- [34] J. Shan, L. Cui, F. Zhou, R. Wang, K. Cui, Y. Zhang, Z. Liu, *ACS Appl. Mater. Interfaces* **2020**, *12*, 11972.
- [35] J. Zhao, M. Shaygan, J. Eckert, M. Meyyappan, M. H. Rummeli, *Nano Lett.* **2014**, *14*, 3064.
- [36] X. Song, J. Liu, L. Yu, J. Yang, L. Fang, H. Shi, C. Du, D. Wei, *Mater. Lett.* **2014**, *137*, 25.
- [37] C. Yang, H. Bi, D. Wan, F. Huang, X. Xie, M. Jiang, *J. Mater. Chem.* **2013**, *1*, 770.
- [38] M. Hiramatsu, K. Shiji, H. Amano, M. Hori, *Appl. Phys. Lett.* **2004**, *84*, 4708.
- [39] K. Shiji, M. Hiramatsu, A. Enomoto, M. Nakamura, H. Amano, M. Hori, *Diamond Relat. Mater.* **2005**, *14*, 831.
- [40] S. C. Xu, T. Cheng, Q. Yan, C. Shen, Y. Yu, C. T. Lin, F. Ding, J. Zhang, *Adv. Sci.* **2022**, *9*, 2200737.
- [41] H. K. Raut, V. A. Ganesh, A. S. Nair, S. Ramakrishna, *Energy Environ. Sci.* **2011**, *4*, 3779.
- [42] Z. W. Han, Z. B. Jiao, S. C. Niu, L. Q. Ren, *Prog. Mater. Sci.* **2019**, *103*, 1.